Available online at www.sciencedirect.com
SCIENCE DIRECT®
Molecular & Biochemical Parasitology 128 (2003) 217–228
MOLECULAR & BIOCHEMICAL PARASITOLOGY

Improvements in transfection efficiency and tests of RNA interference (RNAi) approaches in the protozoan parasite *Leishmania*

Kelly A. Robinson, Stephen M. Beverley*

Department of Molecular Microbiology, Washington University Medical School, 660 S. Euclid Ave., St. Louis, MO 63110, USA

Received 21 January 2003; received in revised form 27 February 2003; accepted 5 March 2003

Abstract

Approaches which eliminate mRNA expression directly are ideally suited for reverse genetics applications in eukaryotic microbes which are asexual diploids, such as the protozoan parasite *Leishmania*. RNA interference (RNAi) approaches have been successful in many species, including the related parasite *Trypanosoma brucei*. For RNAi tests in *Leishmania*, we developed improved protocols for transient and stable DNA transfection, attaining efficiencies of up to 25 and 3%, respectively. This facilitated RNAi tests at the α-tubulin locus, whose inhibition gives a strong lethal phenotype in trypanosomatids. However, transient or stable transfection of DNAs encoding mRNAs for an α-tubulin stem-loop construct and GFP to monitor transfection resulted in no effect on parasite morphology, growth or tubulin expression in *Leishmania major* or *L. donovani*. Transient transfection of a 24-nucleotide double-stranded α-tubulin siRNA also had no effect. Similar results were obtained in studies targeting an introduced GFP gene with a GFP stem-loop construct. These data suggest that typical RNAi strategies may not work effectively in *Leishmania*, and raise the possibility that *Leishmania* is naturally deficient for RNAi activity, like *Saccharomyces cerevisae*. The implications to parasite biology, gene amplification, and genetic analysis are discussed.

Keywords: RNAi; *Leishmania major*; *Leishmania donovani*; Double-stranded RNA; Transient transfection; Genetic analysis

1. Introduction

The protozoan parasite *Leishmania* is the causative agent of leishmaniasis, whose clinical manifestations range from cutaneous skin lesions to the deadly visceral form. *Leishmania* occurs in tropical and sub-tropical regions of the world, with 12 million people infected and another 350 million at risk [1]. The development of molecular and, reverse and forward genetic tools has significantly aided in the study of this organism (reviewed in [2,3]). Together, these methods allow investigators to probe many aspects of parasite biology, including its penchant for molecular and cellular novelty as well as its ability to survive within the phagolysosome of the mammalian macrophage or the gut of its sand fly vector.

Both forward and reverse genetic methods have been hindered by the fact that *Leishmania* is an asexual diploid. The problem is especially acute for forward genetics, since the loss of function mutants occur infrequently, even after powerful mutagenesis ($\sim 10^{-7}$; [4]). Similarly, while gene targeting works extremely efficiently, two rounds are required in order to create null mutants [5]. One attractive alternative involves the use of antisense RNA technologies, which have the virtue of targeting expression from both alleles and/or multiple copies simultaneously, potentially yielding mutants often termed 'knockdowns'. However, antisense RNA strategies have not proven generally effective in *Leishmania*, typically showing small or no effects (for examples, see [6–8]). One striking exception occurred in studies of the *L. donovani* A2 gene, where substantial reduction in A2 expression enabled studies of the role of this gene product in virulence [9].

A strategy for reducing RNA expression termed RNA-interference (RNAi) has shown great promise in genetic analysis of many organisms [10,11]. In this approach,

Abbreviations: RNAi, RNA interference; PI, propidium iodide; GFP+, enhanced green fluorescence protein; siRNA, small interfering RNA; T7nls, T7 nuclear localization signal; dsRNA, double-stranded RNA; HYG, hygromycin phosphotransferase; SAT, nourseothricin; ORF, open reading frame; GFP(65), wild-type GFP; SSU, small subunit of ribosomal RNA

* Corresponding author. Tel.: +1-314-747-2630; fax: +1-314-747-2634.
E-mail address: beverley@borcim.wustl.edu (S.M. Beverley).

0166-6851/03/$ – see front matter © 2003 Elsevier Science B.V. All rights reserved.
doi:10.1016/S0166-6851(03)00079-3

expression of double-stranded RNA leads to specific decreases in the abundance of cognate mRNAs. dsRNA can be delivered in a variety of ways, for example by introduction of large or small dsRNAs directly, or through expression from appropriate expression vectors following transfection (reviewed in [12]). Larger dsRNAs are cleaved into short 21–24 mers (termed small interfering RNAs or siRNAs) by the action of an endogenous RNAse, which then target cognate mRNAs for degradation [12]. Synthetic or pre-formed siRNAs can be directly introduced, eliminating the need for the cleavage/processing step [13].

Since RNAi activity eliminates mRNAs arising from both alleles, or from repetitive genes, it is ideally suited for asexual diploids. In trypanosomes, which are diploids with an experimentally difficult sexual cycle, RNAi has proven a powerful tool for both forward and reverse genetic analysis [14–16]. Given the utility and potential of this approach for genetic analysis of *Leishmania*, we tested the feasibility of classic RNAi approaches to reduce gene expression at multiple *Leishmania* loci. As part of these studies, we developed improved protocols for transient and stable transfection that proved helpful and will facilitate other forms of genetic analysis of *Leishmania*. For the RNAi studies, the use of transient transfections approaches guards against potential problems accompanying stable transfections, which typically use constitutively active expression vectors. Hypothetically, selection for the drug resistance expression could simultaneously select against RNAi-mediated inhibition, especially when targeting essential genes. Transient transfection assays are not subject to this reservation.

2. Materials and methods

2.1. Plasmids

For each construct the relevant regions were confirmed by DNA sequencing.

2.1.1. pXG-P_{LmrRNA}-GFP+

pXG-P_{LmrRNA}-GFP+ (strain B4734; Fig. 1A) contains an *L. major* ribosomal rRNA promoter (P_{LmrRNA}) driving expression of a GC-rich, S65T mutant GFP (termed GFP+; [17]). P_{LmrRNA} was obtained from pR2-Lac2-GFP+ (strain B3095; S. Singer, unpublished data) by digestion with *Nde*I and *Xho*I. The ends of the 3385-bp fragment were filled-in with T4 polymerase and blunt-end ligated into the *Sma*I site of pXG-HYG (strain B3318) [17].

2.1.2. pXG-T7 (B4224)

pXG-T7 (B4224) contains the T7 promoter inserted upstream of the pXG1A (B1495) expression cloning site. The T7 promoter was removed from pBSKII by digestion with *Bss*TII and *Hin*dIII and filled-in with T4 polymerase, and this fragment was ligated into the filled-in *Sal*I site of pXG1A [17].

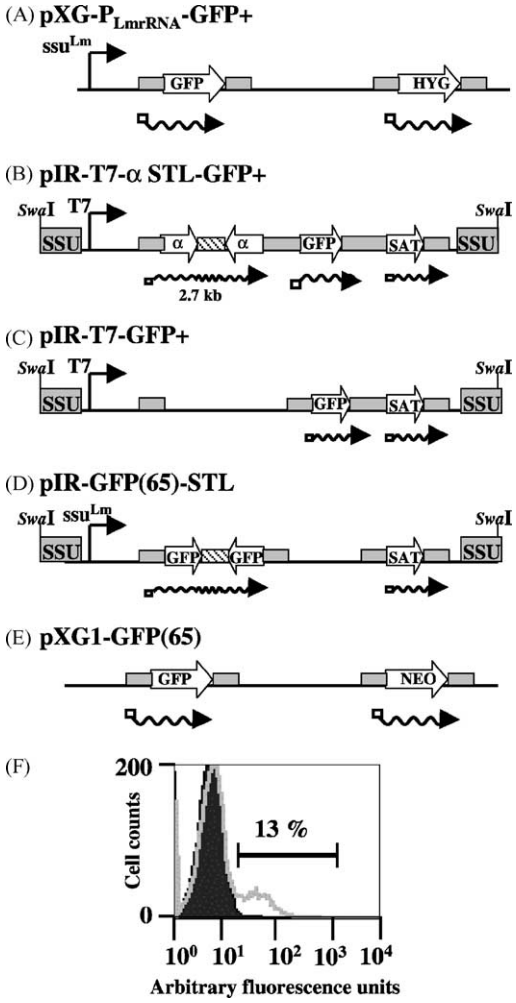

Fig. 1. Features of key plasmid constructs used in this report and flow cytometric analysis of transient transfection. (A) pXG-P_{LmrRNA}-GFP+ expresses mRNAs containing the GFP+ and *HYG* ORFs driven by the *L. major* ribosomal RNA promoter (P_{LmrRNA}). Gray boxes flanking the *HYG* ORF mark *DHFR-TS* 5′ and 3′ flanking sequences supplying splice acceptor and polyadenylation sites required for proper transcript processing. Gray boxes flanking the GFP+ ORF contain the 5′ region of the DST RNAs downstream of *DHFR-TS* and the 5′ region of the 6.2-kb RNA. (B) pIR-T7-αSTL-GFP+ contains an αSTL cassette and the GFP ORF. Both regions are expressed from the T7 promoter in transient transfections. The gray boxes flanking the αSTL represent the DST and the intergenic region of the *L. pifanoi CYS2* ORF. The gray boxes flanking in the GFP+ ORF represent the *CYS2* and the *L. donovani* LPG1 intergenic regions. The *SAT* ORF is flanked by the *LPG1* and the 1.7-kb RNA intergenic regions. *Swa*I sites used to liberate the fragment for integration of this region into the SSU rDNA locus are shown. (C) pIR-T7-GFP+ is the same construct as pIR-T7-αSTL-GFP+ except the αSTL region has been removed. The flanking regions required for processing are the same as described above for pIR-T7-αSTL-GFP+. (D) pIR-GFP(65)-STL contains a GFP stem-loop and *SAT* marker with expression driven by the *L. major* SSU ribosomal promoter. (E) pXG1-GFP(65) contains the GFP(65) ORF and the *NEO* selectable marker. The flanking regions required for processing are the same as described above for pXG-P_{LmrRNA}-GFP+. (F) *L. donovani* cells transiently transfected with pXG-P_{LmrRNA}-GFP+. Seven hours after transfection, cells were washed in 1 × PBS and analyzed by flow cytometry. The filled histogram represents mock transfected cells, while the open histogram represents cells transfected with pXG-P_{LmrRNA}-GFP+. The bar marks cells that were scored as GFP-expressing transfected cells.

2.1.3. pIR-T7-αSTL-GFP+ (B4450; Fig. 1B)

Nucleotides 539–1092 of the *L. major* α-tubulin open reading frame (ORF; GenBank accession number AL359777) were amplified by PCR using *L. major* Friedlin V1 genomic DNA template and primers SMB1314 (5′-agatctCCGGCACGTACCGCC) and SMB 1314 (ggatccGCGCGGGTACGGCAC; lower case refers to added nucleotides). The fragment was ligated into pGEM®-T-Easy to create pTe-α ORF (B4392), and excised from this vector with *Bam*HI and *Bgl*II and ligated into the *Bam*HI site of pXG-T7 (B4224) to create pXG-T7-α (B4393). The 'loop' fragment containing 550 nucleotides of human Pex11β sequence was generated by PCR with primers SMB1259 (5′-agatctTAGCTCCCCGAGTGG) and SMB1260 (5′-agatctAAGATCCTCCTCGG) using plasmid pJM326 DNA [18] as template (Ullu, Yale University). This fragment was cloned into pGEM®-T-Easy to create pTe-stuffer (B4347), liberated with *Bgl*II, and ligated into the *Bam*HI site of pXG-T7-α to create pXG-T7-α-stuffer (B4401). Next, the 553-bp fragment from pTe-α ORF was ligated into the *Bam*HI site of pXG-T7-α stuffer to create pXG-T7-αSTL (B4350). The α-tubulin stem-loop (αSTL) region was obtained from pXG-T7-αSTL by digestion with *Xma*I and *Sac*I, and the 1730-bp fragment was filled-in with T4 polymerase and ligated into the *Sma*I site of pIR1SAT-GFP+(b) (B3538; Hubel, unpublished data) to create pIR-αSTL-GFP+ (B4349). pIR1SAT-GFP+(b) is an expression vector which contains the GFP+ ORF flanked by the *CYS2* and the *L. donovani LPG1* intergenic regions; it also contains the SAT selectable marker flanked by the *LPG1* and the 1.7-kb RNA intergenic regions. The T7 promoter region was removed from pBSK-GFP+ (B2798) by digesting with *Bss*HI and *Hin*dIII. The 70-bp fragment was filled-in and ligated into the filled-in *Mlu*I site of pIR-αSTL-GFP+ to create pIR-T7-αSTL-GFP+ (B4450).

2.1.4. pIR-T7-GFP+ (B4769)

pIR-T7-αSTL-GFP+ was digested with *Xba*I and *Xma*I to remove the αSTL segment, filled in with T4 DNA polymerase, and self-ligated (Fig. 1C).

2.1.5. pTe-α-588 (B4583)

pTe-α-588 (B4583) contains sequences specific for the 3′ region of the *L. major* α-tubulin ORF (GenBank accession number AL359777) not contained in the αSTL construct described above. A PCR fragment containing nucleotides 1095–1653 of the α-tubulin ORF, obtained using primers SMB1452 (5′-CCACTTCGTGCTGACGAGC) and SMB1530 (5′-GTACTCCTCGACGTCCTCCTC), was ligated into pGEM®-T-Easy to create pTe-α-558 (B4583).

2.1.6. pIR-GFP(65)-STL (B4733)

pXS-GFP stem-loop (Ullu, Yale University) contains the unmodified GFP ORF (termed GFP(65) here to distinguish it from GFP+) without an ATG, in a stem-loop configuration. Digestion with *Eco*RI and *Hin*dIII released the 2000-bp stem-loop segment, which was filled-in with T4 polymerase and ligated into a filled-in *Bam*HI site of pIR1SAT (B3541) (Fig. 1D).

2.1.7. pXG1-GFP(65) (B2355; formerly pXG1-GFP [5]; Fig. 1E)

pXG1-GFP(65) (B2355; Fig. 1E) contains the GFP(65) ORF ligated into the *Bam*HI site of pXG1 (B1288) (Fig. 1E).

2.1.8. pX63HYG-T7nls (B678)

pX63HYG-T7nls (B678) contains the T7 polymerase ORF with a nuclear localization signal. The T7 polymerase was obtained by a *Bgl*II/*Bam*HI digest of pAR3283 [19] and ligation into the *Bgl*II site of pX63HYG [5]; strain B617).

2.1.9. siRNA

The double-stranded α-tubulin siRNA 5′-r(CGCGUGCUGGGAGCUGUUCUUU)d(TT) was synthesized (Xeragon Inc.) and resuspended in sterile buffer as supplied by the manufacturer to a final concentration of 40 μM. This siRNA corresponds to nucleotides 54–73 of the α-tubulin ORF (GenBank accession number AL359777). The double-stranded control siRNA 5′-r(UUCUCCGAACGUGUCACGU)d(TT) sequence does not match other current sequences in the *Leishmania* genome database, and was resuspended as above to a final concentration of 20 μM.

2.2. Leishmania strains and transfections

Promastigotes of *L. major* strain Friedlin V1 (MHOM/IL/80/Friedlin) were grown in M199 medium [20]. The *L. donovani* strain LD1S (MHOM/SD/00/1S-2D; Ld-Bob subline) was grown in media described elsewhere (S. Goyard, H. Segawa, J. Gordon, M. Showalter, R. Duncan, S.J. Turco, S.M. Beverley, manuscript submitted). Electroporations were performed by one of the methods described below; for stable transfections, after 1 day of growth in M199 medium cells were plated on semisolid M199 medium additionally bearing selective drugs as appropriate. Following the recommended genetic nomenclature, integration of constructs into the small subunit of the rRNA locus is designated following a colon (*L. major* SSU:GFP+).

L. donovani was transfected with pX63HYG-T7nls and selected on 100 μg/ml of hygromycin B. For *L. major*, expression was obtained following integration of pIR1SAT-T7nls (which had been previously digested with *Swa*I to expose the SSU rRNA targeting sequences) into the rDNA locus after plating on 125 μg/ml nourseothricin. Expression of the T7 polymerase in both *L. donovani* and *L. major* strains was verified using a P_{T7}-*lac*Z construct [21].

L. donovani and *L. major* strains transfected with pXG-P_{LmrRNA}-GFP+ were plated on media containing 14 and 30 μg/ml hygromycin B, respectively. Stable transfectants of *L. major* SSU:T7-αSTL-GFP+ and SSU:GFP(65)-STL were selected on 100 μg/ml of nourseothricin; the latter were subsequently transfected with pXG1-GFP(65) and selected on 30 μg/ml of G418.

For the high-voltage protocol, *Leishmania* was grown to mid-log phase. Cells were pelleted at 1300 × *g* for 10 min and washed in half of the original volume with cytomix electroporation buffer (120 mM KCl_2, 0.15 mM $CaCl_2$, 10 mM K_2HPO_4, 25 mM HEPES, 2 mM EDTA, and $MgCl_2$; pH 7.6) [22]. Cells were pelleted again at 1300 × *g* for 10 min. The pellet was resuspended in cytomix buffer to a final concentration of 2×10^8 cells/ml. Typically, 10 μg of pXG-P_{LmrRNA}-GFP+ was aliquoted into a 4-mm gap cuvette. Next, 500 μl of cells were added to the cuvette and mixed. The cells were electroporated twice at 25 μF, 1500 V (3.75 kV/cm), pausing 10 s between pulses. Transfections conducted with the low-voltage protocol were done as previously described [23]. Briefly, cells were washed and resuspended in electroporation buffer (21 mM HEPES, 137 mM $NaCl_2$, 5 mM KCl_2, 0.7 mM Na_2HPO_4, 6 mM glucose; pH 7.5). In a 2-mm cuvette 400 μl of cells (4.0×10^7 total) were electroporated once at 500 μF, 450 V (2.25 kV/cm) and placed on ice for 10 min. For both protocols, following electroporation cells were transferred to appropriate media (5 or 10 ml for *L. donovani* or *L. major*, respectively) and incubated at 26 °C. PI uptake and GFP expression was monitored at 2 and 7 h post-transfection, respectively, unless otherwise noted. Transfection efficiencies were calculated as the percent of cells electroporated.

2.3. Flow cytometry and immunofluorescence microscopy

For flow cytometry, 750 μl culture aliquots were removed, cells pelleted in a micro-centrifuge at 1300 × *g* for 5 min, and washed once in 1 ml of 1 × PBS-glucose (PBS containing 1% glucose). The cell pellet was resuspended in 500 μl of 1 × PBS-glucose, and PI was added to a final concentration of 50 ng/ml and incubated at room temperature for 5 min. Cells were analyzed for PI uptake (to measure permeabilization at early time points and viability at later times after electroporation) and GFP fluorescence with the Becton Dickinson FACS-Calibur system; GFP was only scored in PI-negative cells. Samples were analyzed under the microscope for the number of GFP-negative and GFP-expressing cells, with normal or "FAT" morphology; this was defined as cells that had a clearly rounded morphology, as opposed to the normal elongated procyclic form. Prior to these analyses, another investigator coded the slides anonymously to ensure objectivity. For each transfection, at least 300 GFP-positive and 300 GFP-negative cells were scored.

2.4. Northern and Western blotting

RNA isolation and Northern blot hybridizations were conducted as described [24] except membranes were pre-hybridized in 10 ml of solution containing 50% formamide, 0.25 M $NaHPO_4$, pH 7.4, 5× Denhardt's solution, 0.5% SDS and 0.1 mg/ml salmon sperm for 2–4 h at 55 °C. Labeled riboprobes (50 μl) were added directly to pre-hybridization solution and incubated overnight at 55 °C. The next day, the membrane was washed three times for 20 min in 2× SSC and 0.1% SDS at 65 °C. RNA probes (cRNA) were synthesized using the Riboprobe® System (Promega) according to manufacturer's directions. cRNA recognizing endogenous α-tubulin mRNA was synthesized using T7 polymerase with *Sac*I-digested pTe-α-588 (B4583) as a template. cRNA recognizing the 'loop' region (Pex11β sequences) was synthesized by SP6 polymerase with *Sph*I-digested pTe-stuffer (B4347) as a template.

2.4.1. Western blots

Leishmania protein extracts and Western blot hybridizations were conducted as previously described [25]. α-Tubulin protein was identified by a 1/10,000 dilution of a mouse monoclonal antibody made against *S. purpuratus* α-tubulin (clone B-5-1-2; Sigma–Aldrich). A 1/2000 dilution of the anti-mouse HRP antibody was used as a secondary antibody (Amersham).

3. Results

3.1. Increased transient transfection efficiencies in Leishmania

A number of experimental parameters were explored in an effort to increase transient transfection efficiencies in *Leishmania*. A reporter plasmid containing the small subunit ribosomal promoter from *L. major* driving expression of a GC-rich S65T GFP mutant (termed GFP+; pXG-P_{LmrRNA}-GFP+; Fig. 1A) was used. Trypanosomatid protozoa synthesize long polycistronic RNA precursors, which are processed by 5′-*trans*-splicing and 3′-polyadenylation to yield monocistronic mRNAs [26]. While inclusion of a promoter is not required for strong expression from episomes in stable transfections of *Leishmania*, it is required for high expression in transient transfections. RNA polymerase I promoters, or a T7 RNA polymerase I promoter in cells expressing T7 RNA polymerase, work effectively [21,27,28].

We initially focused on *L. donovani* as previous studies had shown that transfection efficiencies were higher in this species [29]. As revealed by flow cytometry or fluorescence microscopy, transfection of pXG-P_{LmrRNA}-GFP+ into *L. donovani* using the best transient transfection conditions described below led to the appearance within 7 h of a strongly GFP fluorescent cell population (Figs. 1F and 2A). In contrast, mock transfections result in no GFP expression (Fig. 1F). Similar results were obtained using a T7 RNA polymerase/promoter system, which in this case depended on the presence of both T7 RNA polymerase expression in the recipient cell and a T7 promoter on the transfecting DNA (data not shown).

These studies showed that a high-voltage protocol used with trypanosomes [10] worked effectively in *L. donovani*.

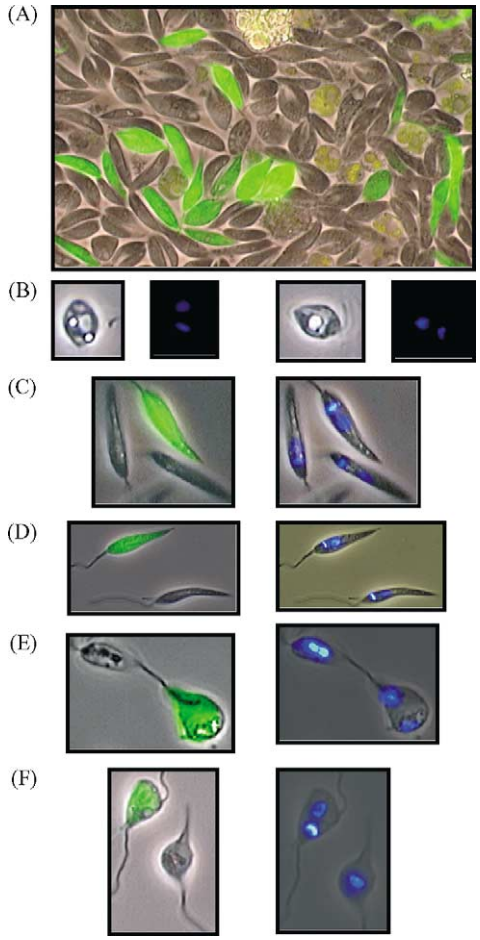

Fig. 2. Expression of GFP in electroporated *Leishmania*. (A) Transient transfection of *L. donovani* with pXG-P_{LmrRNA}-GFP+. (B) *L. major* cells were incubated with 75 μM oryzalin to induce the "FAT-like" morphology, and fixed and stained with Hoescht dye on the following day. (C) *L. major* SSU:T7nls transiently transfected with pIR-T7-αSTL-GFP+ plasmid displaying a normal morphology. (D) *L. major* SSU:T7nls transiently transfected with pIR-T7-GFP+ displaying a normal morphology. (E) *L. major* SSU:T7nls transiently transfected with pIR-T7-αSTL-GFP+ with a "FAT-like" morphology. (F) *L. major* SSU:T7nls transiently transfected with pIR-T7-GFP+ displaying a "FAT-like" morphology.

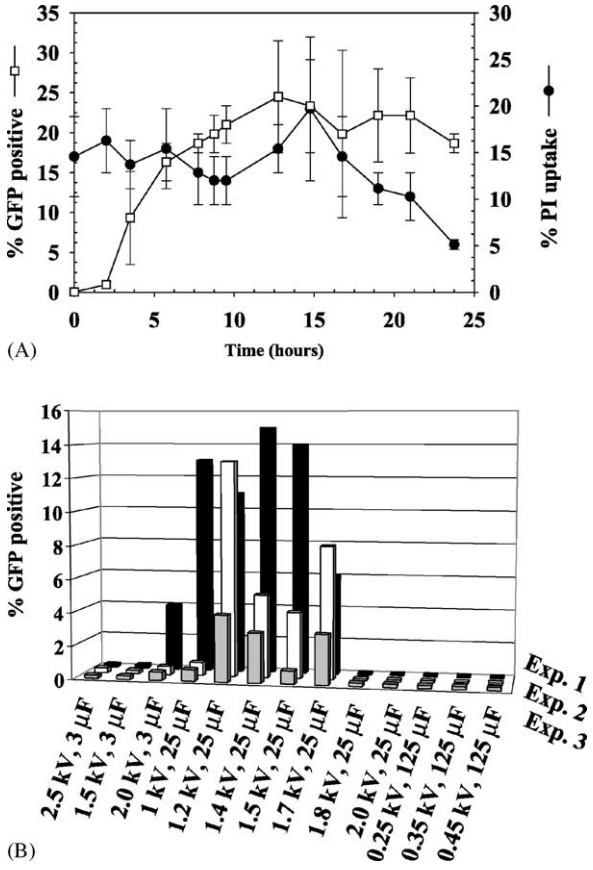

Fig. 3. Factors affecting transient transfection. *L. donovani* was transfected with 10 μg of pXG-P_{LmrRNA}-GFP+ plasmid DNA. (A) Time course of GFP expression and PI uptake for transient transfections using the high-voltage protocol. Aliquots were taken and analyzed by flow cytometry for GFP expression (open square; gated to remove PI+ cells) or PI uptake (closed circle). Error bars show the standard deviation with an $N = 3$. (B) Test of different voltage and capacitance settings on transient transfection efficiencies. The expression of GFP for three separate trials of each combination is shown along the *z*-axis.

With 10 μg of pXG-P_{LmrRNA}-GFP+ DNA, up to 25% of the cells expressed GFP (Fig. 3A). This protocol differed from the low-voltage protocol used previously [23], as cells were resuspended in cytomix buffer [22] and electroporated at a capacitance of 25 μF, applied voltage gradient of 3.75 kV/cm, and in a cuvette with a 4-mm gap width. A time course experiment showed that GFP expression peaked between 7–12 h post-transfection, and was maintained thereafter for at least 24 h (Fig. 3A). The percentage of GFP-positive cells decreased by about 50% after 54 h and declined further thereafter (data not shown). Staining with propidium iodide (PI) was used to monitor permeabilization at the earliest time points, and cellular viability at the later time points (Fig. 3A). Notably, we excluded PI+ cells from the calculations of percent GFP-positive cells obtained by flow cytometry, thus restricting these estimates to viable cells.

Variables including electroporation buffer, voltage and capacitance settings were examined. GFP expression peaked at around 15% with a capacitance of 25 μF and voltage gradients in the range of 3.4–4.4 kV/cm (Fig. 3B). Both the cytomix and the low-voltage protocol electroporation buffers worked equally well (data not shown). Curiously, we found that when the same voltage gradient was applied in a 2-mm cuvette, transfection efficiencies dropped dramatically (data not shown), despite the fact that the electroporation time constant and cell permeabilization (as monitored by PI uptake) were similar to experiments done in 4-mm cuvettes. This unanticipated 'gap effect' may explain why these electroporation conditions were not identified in previous studies using 2-mm cuvettes.

We also explored the effect of DNA concentration and cell number on transient transfection efficiencies. The percent GFP-positive cells obtained following transfection with pXG-P_{LmrRNA}-GFP+ rose with increasing amounts of DNA, until GFP expression plateaued at about 25% with

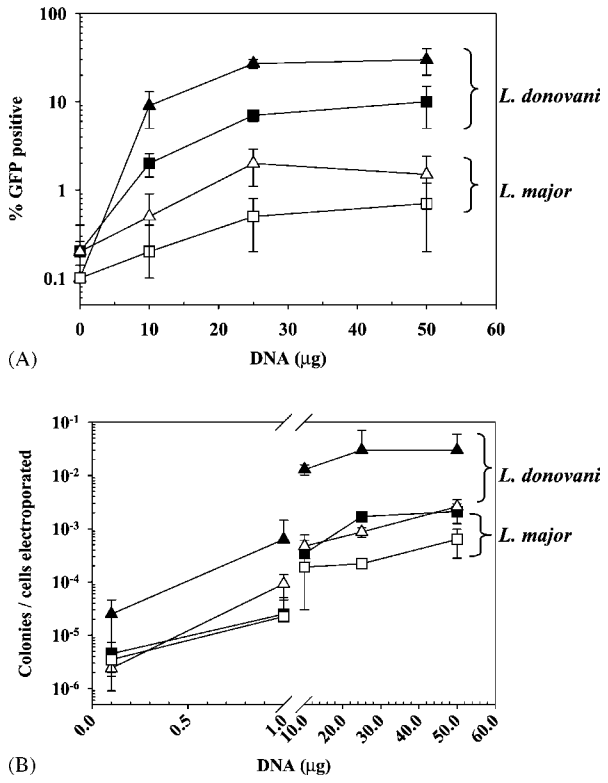

Fig. 4. Transient and stable transfection efficiencies. (A) GFP expression of *L. major* and *L. donovani* transient transfectants using the low- and high-voltage protocols. *L. major* (open symbols) or *L. donovani* (closed symbols) were transfected with increasing amounts of pXG-P_{LmrRNA}-GFP+ using the low (square)- or high (triangle)-voltage conditions. An aliquot of cells was taken 10–16 h post-transfection for FACS analysis. Error bars represent standard deviation with an $N = 3$. (B) Stable transfection efficiencies obtained for *L. major* and *L. donovani* using the low- and high-voltage protocols. Twenty-four hours after transfection, cells were plated onto solid agar plates containing hygromycin B, and colonies were counted 14 days later. Symbols are those shown in panel A and the average and standard deviation for two experiments are shown.

addition of 25 μg of DNA in *L. donovani* (Fig. 4A). Tests with cell numbers ranging from 5.0×10^6 to 1.0×10^8 per electroporation cuvette showed equivalent efficiencies (data not shown).

The high-voltage protocol also increased the transient transfections efficiency more than 10-fold in *L. major* (Fig. 4A). However, the levels obtained were always about 10-fold lower than in *L. donovani*, peaking at 1–2% (Fig. 4A). Efforts to increase this by varying the eletroporation conditions, or using other strains of *L. major*, were unsuccessful (data not shown). Nonetheless, the levels of transient transfections obtained in *L. major* were sufficient for the RNAi tests described below.

3.2. Increased stable transfection efficiencies in L. donovani and L. major

Parasites were transfected with different amounts of pXG-P_{LmrRNA}-GFP+ DNA using the high and low-voltage protocols, and on the following day cells were plated on selective media in order to determine stable transfection efficiencies. For both protocols, the transfection efficiency increased with the amount of DNA electroporated, up to about 10–20 μg DNA as seen in the transient transfection studies (Fig. 4B). At this plateau, the high-voltage protocol gave transfection efficiencies for *L. donovani* of around 3×10^{-2} (colonies per electroporated cell) nearly a 10-fold increase over the low-voltage protocol (Fig. 4B). With *L. major*, stable transfection efficiencies increased to about 2×10^{-3}, again nearly a 10-fold increase over the low-voltage protocol (Fig. 4B).

3.3. Transient expression of an αSTL transcript has no effect on Leishmania

With the improved transfection protocols, we turned to tests of RNAi strategies in *Leishmania*. Initially we targeted the α-tubulin locus, which has proven extremely sensitive to RNAi and results in a strong phenotype [10]. In *Trypanosoma brucei*, loss of α-tubulin results in a rapid cessation of growth and formation of a characteristic "FAT" morphology, accompanied by elevated DNA content due to failure of cytokinesis [10]. Not surprisingly α-tubulin is also essential in *Leishmania* [30] and treatment of *L. major* or *L. donovani* with the α-tubulin inhibitor oryzalin results in a "FAT-like" phenotype in all cells (Fig. 2B). However, while elevated DNA levels and multiple nuclei due to inhibition of cytokinesis were not seen in oryzalin-treated *Leishmania*, parasites bearing multiple flagella were observed (data not shown; [31]).

α-Tubulin dsRNAs were expressed as 'stem-loop' RNAs, which are extremely effective in trypanosome RNAi [10]. The α-tubulin "stem" contained nucleotides 539–1092 of the α-tubulin ORF; this *L. major* α-tubulin segment has 99% nucleotide identity with the same region in *L. donovani*, and we calculated that 81% of potential 24 mers expected to be generated by classic RNAi mechanisms are identical. The "loop" was a fragment of human DNA used previously in trypanosomes [10,18]. The stem-loop segment (αSTL) was then inserted into a derivative of the high-level *Leishmania* expression vector pIR1SAT. In this construct (pIR-T7-αSTL-GFP+; Fig. 1B), the stem-loop segment was flanked by *Leishmania* intergenic regions providing RNA processing signals necessary for the production of stable mRNAs, and inserted upstream of an expression cassette synthesizing a GFP+ mRNA. Upstream of the two αSTL and GFP+ mRNAs, a T7 RNA polymerase promoter was inserted to drive high-level expression in transient transfections.

Both pIR-T7-αSTL-GFP+ and a GFP expression construct control (pIR-T7-GFP+; Fig. 1C) were introduced transiently into T7 RNA polymerase-expressing *L. major* and *L. donovani* using the high-voltage protocol. After 24 or 48 h, cells were fixed and examined under the microscope for "FAT-like" morphology and GFP expression. As seen

in the transient transfections above, where expression was driven by the rRNA promoter, the percent cells expressing GFP was high (typically, 14 or 1.4% for *L. donovani* and *L. major*, respectively), establishing the activity of the T7 promoter/RNA polymerase system.

In all transfections, there was a background of "FAT-like" cells, which was higher in *L. donovani* than *L. major*, presumably arising from stresses associated with electroporation. However, "FAT-like" cells occurred at a similar frequency in GFP-negative (untransfected) and GFP-expressing (transfected) cells (Fig. 2C–F); quantitatively, this was shown by determination of "FAT cell ratios" (% FAT-like cells in GFP-expressing transfected versus untransfected cells), which were always about 1 (Fig. 5). Similarly, a constant level of multi-flagellated cells of around 5% was observed in all cells, regardless of the specific DNA or whether GFP expression was observed (data not shown). We also examined the GFP-expressing transfected cells for changes in the number of nuclei or kinetoplasts by microscopy following staining with Hoechst 33342 dye (Fig. 2C–F), or for changes in total DNA content by flow cytometry (data not shown). None of these approach showed significant differences between cells transfected with pIR-T7-GFP+ or pIR-T7-αSTL-GFP+, in either the GFP-expressing or GFP-null cell populations.

3.4. Stable expression of αSTL transcript has no effect on *Leishmania* or α-tubulin expression

Since none of the effects expected for inhibition of tubulin expression were observed in transient transfections, we stably expressed the αSTL construct in wild-type *L. major*. The αSTL-GFP+ cassette in pIR-αSTL-GFP+ is flanked by 1-kb segments of the SSU rRNA gene (Fig. 1B), and linearization of this vector with *Swa*I allows these segments to target integration specifically into the rDNA locus. At this site, high levels of gene expression are mediated through transcription by RNA polymerase I (Hubel & Beverley, unpublished data; [32]). *L. major* SSU:αSTL-GFP+ transfectants were obtained at normal frequencies, and transfectants had similar levels of GFP expression by flow cytometry (data not shown). Both the *L. major* SSU:GFP+ and *L. major* SSU:αSTL-GFP+ stable transfectants had normal morphology, and grew normally to comparable densities (data not shown).

The expression of the endogenous α-tubulin mRNA in the αSTL-GFP+ transfectants was assessed by Northern blot analysis with a riboprobe specific for the 3′ end of the α-tubulin ORF (this region is not present in the αSTL construct). The *L. major* SSU:αSTL-GFP+ transfectants had unaltered levels of the endogenous α-tubulin transcript compared to untransfected *L. major* (Fig. 6B). Western blots with α-tubulin antisera also showed no decrease in α-tubulin protein levels, in agreement with the Northern blot data (Fig. 6C).

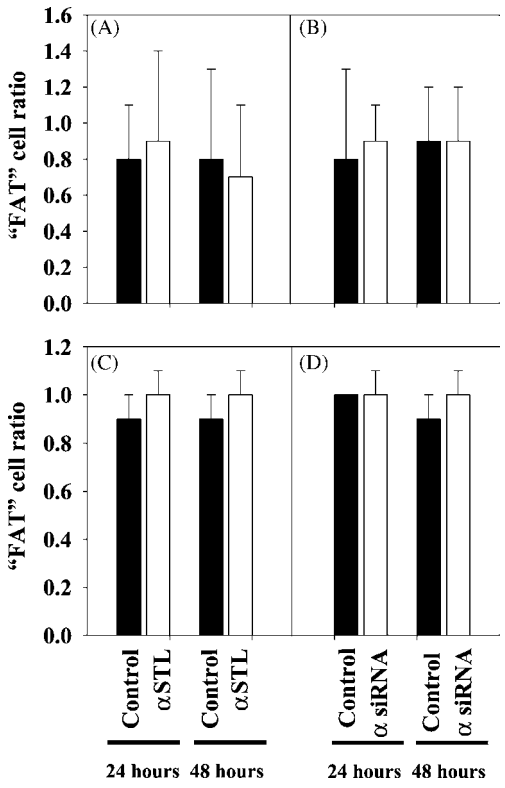

Fig. 5. Analysis of cell morphology for cells transfected with αSTL construct or siRNA. (A) *L. major* SSU:T7nls was transfected with 25 μg of either pIR-T7-GFP+ or pIR-T7-αSTL-GFP+. Twenty-four and 48 h post-transfection cells were fixed and viewed by microscopy. Cells were scored for whether they were had "FAT" or wild-type morphologies, and the ratio of GFP-expressing (transfected) to GFP-negative (untransfected) "FAT" cells was determined and plotted as the "FAT cell ratio". Closed bars represent cells transfected with the control vector pIR-T7-GFP+, open bars represent cells transfected with pIR-T7-αSTL-GFP+. (B) *L. major* SSU:T7nls was transfected with 25 μg pIR-T7-GFP+ and 25 μg of either the control siRNA (closed bars) or α-tubulin siRNA (open bars), and assayed as in panel A. (C) *L. donovani*-pX63HYG-T7nls was transfected with either pIR-T7-GFP+ (closed bars) or pIR-T7-αSTL-GFP+ (open bars) and assayed as in panel A. (D) *L. donovani*-pX63HYG-T7nls was transfected with 25 μg of pIR-T7-GFP+ and either 25 μg of control siRNA (closed bars) or α-tubulin siRNA (open bars), and assayed as discussed above. Error bars for *L. major* transfectants (A, B) represent the standard deviation with an $N = 3$. Error bars for *L. donovani* transfectants (C, D) represent the standard deviation with an $N = 2$. The background of "FAT" cells in these experiments was about 30 and 80% for *L. major* and *L. donovani*, respectively. This arises from the stress of electroporation alone (data not shown).

Expression of the αSTL RNA was established by Northern blot hybridization, using an antisense riboprobe specific for the foreign loop sequences present in the αSTL transcript. These experiments showed multiple mRNAs, which were absent in control parasites (Fig. 6A). The size of one RNA was 2.7 kb (Fig. 6A), which is that predicted for the STL transcript assuming that the *L. major* flanking sequences were correctly recognized and processed (Fig. 1). All independent stable *L. major* SSU:αSTL-GFP+ transfectants expressed a similar pattern of antisense 'loop' RNAs, although the levels varied

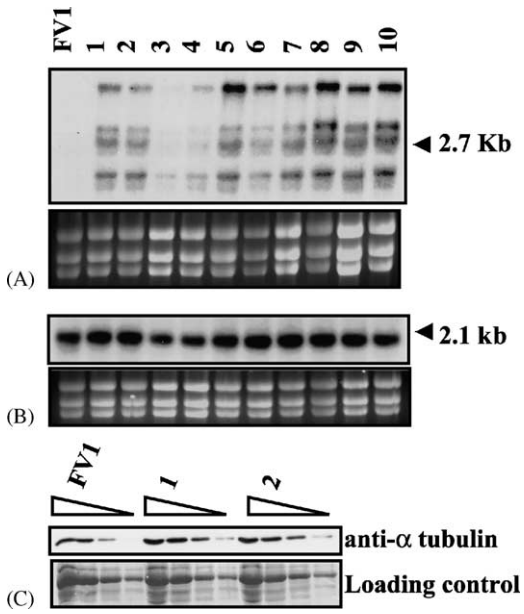

Fig. 6. Expression of αSTL RNAs, α-tubulin mRNA and tubulin protein levels in wild-type and stable SSU:αSTL-GFP+ transfectants. (A) Northern blot to detect the αSTL transcript using a riboprobe specific for loop region is shown (Section 2). The size of the expected 2.7-kb mRNA is marked. Ethidium bromide staining of the gel is shown below the blot as a loading control. (B) Northern blot to detect the endogenous 2.1-kb α-tubulin mRNA. (C) Western blot analysis of α-tubulin protein levels. Lanes marked "FV1" represent two-fold serial dilutions of wild-type *L. major* strain Friedlin protein extracts, while lanes marked "1" or "2" represent similar two-fold dilution series of two clonal lines of *L. major* SSU:αSTL-GFP+ (starting at 5×10^7 cells). Ponceau staining is shown for a loading control.

somewhat (Fig. 6A). The source of the heterogeneity was not investigated, since neither tubulin protein nor mRNAs were affected.

Thus, despite abundant expression of the αSTL RNA in *Leishmania*, no effect on parasite growth or tubulin expression was obtained. Since the transient expression studies above used the same αSTL-GFP+ DNA expression cassettes, and showed good expression of GFP, we infer that expression of the αSTL transcript likely occurred in those studies as well.

3.5. Transient introduction of an siRNA to α-tubulin

The inhibitory effects of RNAi are thought to be mediated following the formation of siRNAs, and these can be introduced directly into cells to eliminate gene expression [13]. However, preliminary Northern blot studies did not reveal the formation of α-tubulin siRNAs in the lines stably expressing the αSTL construct above (data not shown), raising the possibility that *Leishmania* might be deficient in the machinery required to generate siRNAs. To by-pass this step, we introduced an α-tubulin siRNA transiently using the high-voltage electroporation conditions. The siRNA was a double-stranded 24 mers containing two dT residues at the 3′ end [33,34], and whose sequence was identical to nucleotides 54–73 of both the *L. major* and *L. donovani* α-tubulin ORFs. A control siRNA contained sequences that were not homologous to α-tubulin or any sequences currently in the *Leishmania* database. *L. major* and *L. donovani* were electroporated in the presence of 3.4 mM α-tubulin or 3.0 mM control siRNA, simultaneously with 25 mg of pXG-P_{LmrRNA}-GFP+ to identify transfectants. However, there was no significant difference between α-tubulin or control siRNA populations at 24 or 48 h post-transfection, whether or not transfected successfully as revealed by GFP expression, in any phenotype including the appearance of the "FAT" cell morphology (Fig. 5; data not shown). While potentially other siRNAs could be tested, the lack of siRNA formation in the stable αSTL transfectants suggested that this was likely to be fruitless.

3.6. Stable expression of a GFP stem-loop transcript has no effect on GFP expression levels

Since different genes are variably susceptible to RNAi [18,35], we tested other loci. As GFP has been shown to be an effective target of RNAi strategies in both trypanosomes and other organisms, we tested the effect of expressing GFP

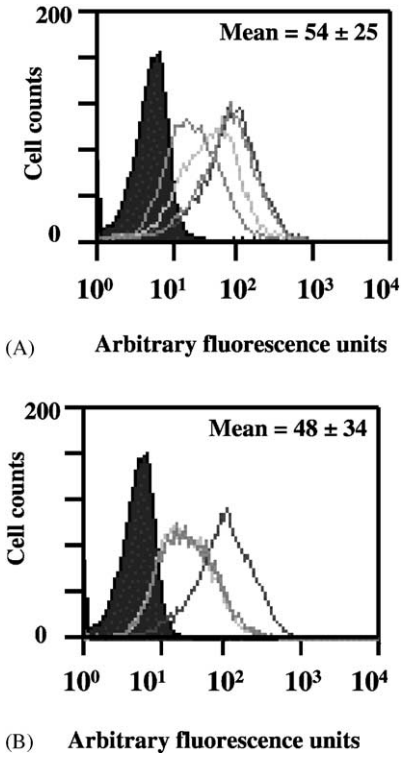

Fig. 7. Flow cytometry of reporter plasmid GFP(65) expression in *L. major* expressing a GFP(65) stem-loop construct. Filled-in histogram shows the background fluorescence of the recipient cells. Four individual transfectant clones for each recipient line are shown, and the mean and standard deviation of GFP expression for these is included in the figure.

in cells engineered previously to express a GFP stem-loop (GFP-STL) construct. These studies used a wild-type GFP (here termed GFP(65)) and a GFP(65)-STL construct similar to that used successfully in RNAi studies in trypanosomes (Ullu, personal communication). The GFP(65)-STL construct contained two copies of the entire GFP(65) ORF (minus the initiating ATG) in an inverted orientation, separated by 600 nucleotides of random stuffer DNA, inserted into the pIR1SAT vector (Fig. 1D). This construct was integrated into the rDNA locus of *L. major* to achieve high levels of expression of the GFP(65)-STL RNA; transfectants were obtained at expected frequencies and grew normally.

Then, wild-type or the *L. major* SSU:GFP(65)-STL parasites were transfected with an episomal pXG-GFP(65) expression vector (Fig. 1E). After recovery of independent clonal transfectant lines, GFP expression was monitored by flow cytometry. Since episomal vectors typically show copy number variation among clones, we examined four clones from the transfectants of WT or SSU:GFP(65)-STL. In keeping with the tubulin studies above, the average fluorescence was not significantly different (54 ± 25 versus 48 ± 34, respectively, for WT versus *L. major* SSU:GFP(65)-STL; Fig. 7).

4. Discussion

In this work, we developed improved methods for transient and stable transfection of *Leishmania*, achieving frequencies of 25 and 3%, respectively, for transient and stable transfection of *L. donovani* (Fig. 4). While the absolute frequencies were about 10-fold less in *L. major*, for both species efficiencies were greatly increased over that achieved previously (Fig. 4). These improvements will greatly facilitate methods such as gene replacement and the generation of large transfection libraries necessary for various functional expression and rescue strategies. Moreover, transient transfection strategies have not been widely utilized in *Leishmania* previously because of the poor efficiencies. However, the efficiencies attained here are sufficient to permit the application of many useful transient approaches, for example probing the targeting of proteins expressed by *Leishmania*.

We used these advances to test for RNAi activity in *Leishmania*. Our most stringent studies focused on α-tubulin, which had been used previously as a strong RNAi 'reporter' in trypanosomes since α-tubulin is essential and its loss results in an easily scorable "FAT" phenotype [10] (Fig. 2B). We first tested the standard "stem-loop" strategy in both transient and stable transfections. The test construct encoded two mRNAs, one an *L. major* αSTL construct and the second a GFP+ reporter, each flanked by *Leishmania* sequences necessary for processing and formation of stable mRNAs (Fig. 1B). In transient transfectants, a T7 promoter drove abundant expression of both the αSTL and GFP+ genes. GFP-positive transfectants arising from pIR-T7-GFP+ or pIR-T7-αSTL-GFP+ showed no significant differences in any phenotype associated with inhibition of α-tubulin expression. Remarkably, we were able to readily obtain stable transfectants which expressed high levels of the αSTL RNA, yet which still grew normally and synthesized normal levels of endogenous α-tubulin mRNA and protein (Fig. 6). Using transient transfections, we also tested the anticipated intermediates of the RNAi pathway, short interfering (siRNAs), again without any morphological or growth phenotypes in cells cotransfected with a GFP+ reporter (Fig. 5).

In a less exhaustive test of RNAi in stable transfections, we targeted expression of a nonessential GFP reporter by expression of a GFP stem-loop construct. Again, we did not observe any attenuation of GFP expression (Fig. 7), in contrast to results obtained in trypanosomes [35]. We also have not had success with efforts targeting the *L. major LPG1* gene (data not shown). These data suggest that classic strategies of RNAi applied successfully in other organisms, including trypanosomes, do not function effectively in *Leishmania*. Significantly, experiments in trypanosomes showed that most if not all RNAi constructs are able to decrease mRNA levels, although sometimes this does not lead to reduced protein levels or detectable phenotypes [18,36,37]. Therefore, the lack of an effect on the endogenous α-tubulin mRNA levels is perhaps the strongest evidence against the efficacy of RNAi in *Leishmania*.

Our studies incorporated controls and a diversity of approaches and targets that give some credibility to the negative outcome. The development and use of transient transfection approaches also avoids one potential artifact, arising from concerns about simultaneous selection for the resistance marker and against RNAi activity. In spite of this, it is possible that some unanticipated experimental or unique property of a hypothetical RNAi pathway in *Leishmania* was not taken into consideration, precluding success. These might include the GC richness of the *Leishmania* genome (approximately 62% GC) and the cellular site or targeting of stem-loop RNA expression; both factors have been shown to modulate (but not nullify) RNAi activity in other organisms [36,38]. We believe that we can rule out a number of variables, for example those associated with the specific gene targeted, or level of expression of the 'RNAi' constructs, as we used the most powerful expression systems available. Moreover, our findings are in keeping with other studies in this organism. Notably, in stable expression of 'stem-loop' A2 RNA was not effective in down-regulating mRNA expression in *L. donovani*, while an antisense approach was successful, and it was concluded that an RNAi-type mechanism was not operative [9,39]. The lack of success of RNAi approaches in *Leishmania* has also been particularly evident in recent scientific meetings in this field, in contrast to its efficacy in trypanosomes [40].

One of the hallmarks of RNAi in other organisms is the formation of siRNAs which then participate in the destruction of mRNAs [12,41]. A number of other biological phenomena have been shown to utilize siRNAs, including

chromatin organization, programmed DNA rearrangements, regulation of mRNA levels and translation, and protective genome surveillance against viruses and transposable elements [12]. The lack of RNAi activity on gene expression in *Leishmania* does not necessarily imply that other related phenomena do not occur in this species, as data are currently lacking. Curiously, a role for RNAi in genome surveillance has been found in *T. brucei*, where RNAi pathways play an important role in modulating the expression of transcripts arising from several abundant transposable element families [42]. Remarkably, the *Leishmania* genome is deficient in such elements ([43] and references cited therein), making the apparent lack of RNAi activity paradoxical.

Nonetheless, the available data raise the possibility that, like a limited number of other species (such as *Saccharomyces cerevisae*), *Leishmania* may be naturally deficient in classic RNAi activity. The forces leading to the loss of RNAi activity in any species are unknown at present. Several observations in *Leishmania* however are consistent with this proposal. First, database searches of the current *Leishmania* genome sequence databases have not identified convincing homologs of genes implicated specifically in RNAi in other organisms. This tentative conclusion will be subject to more stringent tests once the *Leishmania* genome is completed, and the genes responsible for RNAi activity in trypanosomes identified and their homologs sought in *Leishmania*.

A second argument consistent with the "RNAi-null" model is the finding that, in a number of circumstances, *Leishmania* appear to express significant levels of endogenous dsRNAs without any deleterious effect. In wild-type parasites, stable antisense RNAs have been identified for *DHFR-TS* and histone 1 ([44]; Fasel, personal communication), and an antisense EST has been found for the *SCG* loci [45]. Antisense transcription and transcripts have been found frequently from episomal transfectant [46] or amplified DNAs, which occur in a number of drug-resistant *Leishmania* lines [44,47,48]. Lastly, a number of *Leishmania* strains contain a dsRNA virus-like element at high levels [49,50]. Collectively, these data point to a remarkable tolerance of the *Leishmania* parasite to the presence of dsRNAs in many different forms. Notably, reports of simultaneous antisense transcripts and/or transcription are rare in trypanosomes and dsRNA viruses have not been reported.

The apparent lack of RNAi activity in *Leishmania* relative to trypanosomes potentially provides an explanation for a puzzling observation about the occurrence of gene amplification in these species. While *Leishmania* readily undergo extra-chromosomal gene amplification [51], this has not been found in trypanosomes [51]. Similarly, while episomes arising from transfections of circular constructs have been reported in *T. brucei*, they are uncommon and exhibit peculiar properties with respect transcription [52], or consist entirely of repetitive DNA without detectable transcripts (K. Ersfeld, personal communication; [53]). Given the similarities in overall chromosomal organization and transcriptional mechanisms, it has been difficult to understand why *Leishmania* and African trypanosomes would be different. We propose that the differential tolerance of these organisms to the presence of dsRNA, presumably arising from the absence of an RNAi pathway in *Leishmania*, may be responsible for this discrepancy. In this model, in trypanosomes but not *Leishmania*, expression of 'sense' mRNAs from prospective amplified DNAs would be abolished by RNAi activity, arising from dsRNAs generated from "antisense" strand transcription of the amplified DNA. This would preclude the recovery of amplified DNAs encoding genes whose overexpression was essential for survival under drug pressure, for example. Thus, the tolerance of *Leishmania* for dsRNAs, presumably arising from a deficiency in RNAi activity, makes these parasites permissive for episomal DNAs, which commonly exhibit dsRNA transcripts and/or transcription. Several of the predictions of this speculative model can be tested in future studies.

At present, the potential for RNAi-based applications in *Leishmania* genetics appears to be limited, based upon the studies reported here as well as those of others [39,40]. These results imply that other solutions will be necessary to solve the 'diploidy' challenge of forward genetics in *Leishmania*.

Acknowledgements

We thank Elisabetta Ullu for assistance with transient transfection approaches and discussions, Naomi Morrissette for oryzalin, K. Ersfeld and N. Fasel for permission to mention unpublished data, members of the Beverley lab for discussions, and A. Capul, D.E. Dobson, M. Drew, L-F. Lye, R. Matlib, and K. Zhang for comments on this manuscript. Supported by NIH research fellowship (AI50339) to KAR and NIH grant AI 29646 to SMB.

References

[1] Herwaldt BL. Leishmaniasis. Lancet 1999;354:1191–9.
[2] Beverley SM. Genetic and genomic approaches to the analysis of *Leishmania* virulence. In: Marr JM, Nilsen T, Komuniecki R, editors. Molecular & medical parasitology. New York: Academic Press; 2003.
[3] Clayton CE. Genetic manipulation of kinetoplastida. Parasitol Today 1999;15:372–8.
[4] Gueiros-Filho FJ, Beverley SM. Trans-kingdom transposition of the *Drosophila* element *mariner* within the protozoan *Leishmania*. Science 1997;276:1716–9.
[5] Cruz A, Coburn CM, Beverley SM. Double targeted gene replacement for creating null mutants. Proc Natl Acad Sci USA 1991;88:7170–4.
[6] Lye LF, Cunningham ML, Beverley SM. Characterization of *quinonoid*-dihydropteridine reductase (*QDPR*) from the lower eukaryote *Leishmania major*. J Biol Chem 2002;277:38245–53.
[7] Somanna A, Mundodi V, Gedamu L. Functional analysis of cathepsin B-like cysteine proteases from *Leishmania donovani* complex. Evidence for the activation of latent transforming growth factor beta. J Biol Chem 2002;277:25305–12.

[8] Chen DQ, Kolli BK, Yadava N, Lu HG, Gilman-Sachs A, Peterson DA, et al. Episomal expression of specific sense and antisense mRNAs in *Leishmania amazonensis*: modulation of gp63 level in promastigotes and their infection of macrophages in vitro. Infect Immun 2000;68:80–6.

[9] Zhang WW, Matlashewski G. Loss of virulence in *Leishmania donovani* deficient in an amastigote-specific protein, A2. Proc Natl Acad Sci USA 1997;94:8807–11.

[10] Ngo H, Tschudi C, Gull K, Ullu E. Double-stranded RNA induces mRNA degradation in *Trypanosoma brucei*. Proc Natl Acad Sci USA 1998;95:14687–92.

[11] Fire A, Xu S, Montgomery MK, Kostas SA, Driver SE, Mello CC. Potent and specific genetic interference by double-stranded RNA in *Caenorhabditis elegans*. Nature 1998;391:806–11.

[12] Hannon GJ. RNA interference. Nature 2002;418:244–51.

[13] Yu JY, DeRuiter SL, Turner DL. RNA interference by expression of short-interfering RNAs and hairpin RNAs in mammalian cells. Proc Natl Acad Sci USA 2002;99:6047–52.

[14] Bastin P, Ellis K, Kohl L, Gull K. Flagellum ontogeny in trypanosomes studied via an inherited and regulated RNA interference system. J Cell Sci 2000;113(Pt 18):3321–8.

[15] Morris JC, Wang Z, Drew ME, Englund PT. Glycolysis modulates trypanosome glycoprotein expression as revealed by an RNAi library. EMBO J 2002;21:4429–38.

[16] Wang Z, Englund PT. RNA interference of a trypanosome topoisomerase II causes progressive loss of mitochondrial DNA. EMBO J 2001;20:4674–83.

[17] Ha DS, Schwarz JK, Turco SJ, Beverley SM. Use of the green fluorescent protein as a marker in transfected *Leishmania*. Mol Biochem Parasitol 1996;77:57–64.

[18] Wang Z, Morris JC, Drew ME, Englund PT. Inhibition of *Trypanosoma brucei* gene expression by RNA interference using an integratable vector with opposing T7 promoters. J Biol Chem 2000;275:40174–9.

[19] Dunn JJ, Krippl B, Bernstein KE, Westphal H, Studier FW. Targeting bacteriophage T7 RNA polymerase to the mammalian cell nucleus. Gene 1988;68:259–66.

[20] Coderre JA, Beverley SM, Schimke RT, Santi DV. Overproduction of a bifunctional thymidylate synthetase-dihydrofolate reductase and DNA amplification in methotrexate-resistant *Leishmania tropica*. Proc Natl Acad Sci USA 1983;80:2132–6.

[21] LeBowitz JH, Smith HQ, Rusche L, Beverley SM. Coupling of poly(A) site selection and trans-splicing in *Leishmania*. Genes Dev 1993;7:996–1007.

[22] van den Hoff MJ, Moorman AF, Lamers WH. Electroporation in intracellular buffer increases cell survival. Nucleic Acids Res 1992;20:2902.

[23] Kapler GM, Coburn CM, Beverley SM. Stable transfection of the human parasite *Leishmania major* delineates a 30-kilobase region sufficient for extrachromosomal replication and expression. Mol Cell Biol 1990;10:1084–94.

[24] Cunningham ML, Beverley SM. Pteridine salvage throughout the *Leishmania* infectious cycle: implications for antifolate chemotherapy. Mol Biochem Parasitol 2001;113:199–213.

[25] Lemley C, Yan S, Dole VS, Madhubala R, Cunningham ML, Beverley SM, et al. The *Leishmania donovani* LD1 locus gene *ORFG* encodes a biopterin transporter (BT1). Mol Biochem Parasitol 1999;104:93–105.

[26] Clayton CE. Control of gene expression in trypanosomes. Prog Nucleic Acids Res Mol Biol 1992;43:37–66.

[27] Lee MG, Van der Ploeg LH. Transcription of protein-coding genes in trypanosomes by RNA polymerase I. Annu Rev Microbiol 1997;51:463–89.

[28] Gay LS, Wilson ME, Donelson JE. The promoter for the ribosomal RNA genes of *Leishmania chagasi*. Mol Biochem Parasitol 1996;77:193–200.

[29] Ryan KA, Dasgupta S, Beverley SM. Shuttle cosmid vectors for the trypanosomatid parasite *Leishmania*. Gene 1993;131:145–50.

[30] Curotto de Lafaille MA, Wirth DF. Creation of null/+ mutants of the α-tubulin gene in *Leishmania enriettii* by gene cluster deletion. J Biol Chem 1992;267:23839–46.

[31] Chan MM, Triemer RE, Fong D. Effect of the anti-microtubule drug oryzalin on growth and differentiation of the parasitic protozoan *Leishmania mexicana*. Differentiation 1991;46:15–21.

[32] Breitling R, Klingner S, Callewaert N, Pietrucha R, Geyer A, Ehrlich G, et al. Non-pathogenic trypanosomatid protozoa as a platform for protein research and production. Protein Exp Purif 2002;25:209–18.

[33] Zamore PD, Tuschl T, Sharp PA, Bartel DP. RNAi: double-stranded RNA directs the ATP-dependent cleavage of mRNA at 21–23 nucleotide intervals. Cell 2000;101:25–33.

[34] Elbashir SM, Lendeckel W, Tuschl T. RNA interference is mediated by 21- and 22-nucleotide RNAs. Genes Dev 2001;15:188–200.

[35] LaCount DJ, Bruse S, Hill KL, Donelson JE. Double-stranded RNA interference in *Trypanosoma brucei* using head-to-head promoters. Mol Biochem Parasitol 2000;111:67–76.

[36] Ullu E, Djikeng A, Shi H, Tschudi C. RNA interference: advances and questions. Philos Trans R Soc Lond B Biol Sci 2002;357:65–70.

[37] Shi H, Djikeng A, Mark T, Wirtz E, Tschudi C, Ullu E. Genetic interference in *Trypanosoma brucei* by heritable and inducible double-stranded RNA. RNA 2000;6:1069–76.

[38] Holen T, Amarzguioui M, Wiiger MT, Babaie E, Prydz H. Positional effects of short interfering RNAs targeting the human coagulation trigger tissue factor. Nucleic Acids Res 2002;30:1757–66.

[39] Zhang WW, Matlashewski G. Analysis of antisense and double stranded RNA downregulation of A2 protein expression in *Leishmania donovani*. Mol Biochem Parasitol 2000;107:315–9.

[40] Beverley SM. Protozomics: trypanosomatid parasite genetics comes of age. Nat Rev Genet 2003;4:11–9.

[41] Hammond SM, Bernstein E, Beach D, Hannon GJ. An RNA-directed nuclease mediates post-transcriptional gene silencing in *Drosophila* cells. Nature 2000;404:293–6.

[42] Djikeng A, Shi H, Tschudi C, Ullu E. RNA interference in *Trypanosoma brucei*: cloning of small interfering RNAs provides evidence for retroposon-derived 24–26-nucleotide RNAs. RNA 2001;7:1522–30.

[43] Bringaud F, Garcia-Perez JL, Heras SR, Ghedin E, El-Sayed NM, Andersson B, et al. Identification of non-autonomous non-LTR retrotransposons in the genome of *Trypanosoma cruzi*. Mol Biochem Parasitol 2002;124:73.

[44] Kapler GM, Beverley SM. Transcriptional mapping of the amplified region encoding the dihydrofolate reductase-thymidylate synthase of *Leishmania major* reveals a high density of transcripts, including overlapping and antisense RNAs. Mol Cell Biol 1989;9:3959–72.

[45] Dobson DE, Scholtes L, Valdez K, Sullivan DR, Mengeling BJ, Cilmi S, et al. Functional identification of galactosyltransferases (SCGs) required for species-specific modifications of the lipophosphoglycan (LPG) adhesin controlling *Leishmania major*–sand fly interactions. J Biol Chem 2003;278:15523–31.

[46] Wong AK, Curotto de Lafaille MA, Wirth DF. Identification of a *cis*-acting gene regulatory element from the *lemdr1* locus of *Leishmania enriettii*. J Biol Chem 1994;269:26497–502.

[47] Belli S, Formenton A, Noll T, Ivens A, Jacquet R, Desponds C, et al. *Leishmania major*: histone H1 gene expression from the *sw3* locus. Exp Parasitol 1999;91:151–60.

[48] Tripp CA, Wisdom WA, Myler PJ, Stuart KD. A multicopy extrachromosomal DNA in *Leishmania infantum* contains two inverted repeats of the 275-kilobase LD1 sequence and encodes numerous transcripts. Mol Biochem Parasitol 1992;55:39–50.

[49] Tarr PI, Aline Jr RF, Smiley BL, Scholler J, Keithly J, Stuart K. LR1: a candidate RNA virus of *Leishmania*. Proc Natl Acad Sci USA 1988;85:9572–5.
[50] Widmer G, Comeau AM, Furlong DB, Wirth DF, Patterson JL. Characterization of a RNA virus from the parasite *Leishmania*. Proc Natl Acad Sci USA 1989;86:5979–82.
[51] Borst P, Ouellette M. New mechanisms of drug resistance in parasitic protozoa. Annu Rev Microbiol 1995;49:427–60.
[52] Patnaik PK, Kulkarni SK, Cross GA. Autonomously replicating single-copy episomes in *Trypanosoma brucei* show unusual stability. EMBO J 1993;12:2529–38.
[53] Alsford NS, Navarro M, Jamnadass HR, Dunbar H, Ackroyd M, Murphy NB, et al. The identification of circular extrachromosomal DNA in the nuclear genome of *Trypanosoma brucei*. Mol Microbiol 2003;47:277–89.